Results in Engineering 27 (2025) 105646

Contents lists available at ScienceDirect

Results in Engineering

journal homepage: www.sciencedirect.com/journal/results-in-engineering

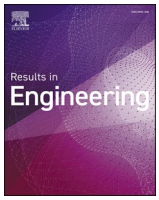

Prediction and analysis of punching shear capacity in steel fiber reinforced concrete slab using machine learning

XuanRui Yu [a], Nima Khodadadi [b,*], Anxiang Song [c,*], Yang Yu [d], Antonio Nanni [b]

[a] School of Civil Engineering. Chongqing University of Science and Technology, Shapingba District, Chongqing 401331, PR China
[b] Department of Civil and Architectural Engineering, University of Miami, Coral Gables, FL 33146, USA
[c] Department of Civil Engineering, Chongqing Three Gorges University, Wanzhou, Chongqing, 404100, PR China
[d] Centre for infrastructural Engineering and Safety, School of Civil and Environmental Engineering The University of New South Wales, High Street, Sydney 2052. Australia

ARTICLE INFO

Keywords:
Steel Fiber
Concrete Slab
Punching Shear Capacity
Machine Learning
Variable Importance

ABSTRACT

The study of punching shear capacity in steel fiber reinforced concrete (SFRC) slabs is significant for enhancing the safety of slab-type structures. It helps engineers optimize structural designs and ensures the stability of buildings under various loading conditions. Although numerous models have been proposed to predict punching shear capacity, their limited consideration of influencing factors often results in low prediction accuracy, making them insufficient for practical engineering applications. This study proposes a Backpropagation Neural Network (BPNN) model optimized by the Grey Wolf Optimizer (GWO) to improve prediction performance. By optimizing the initial weights and biases of the network, the model achieves faster convergence and higher predictive accuracy, effectively capturing the complex nonlinear relationships among input variables. The input features include slab thickness, effective depth, loading pad length, and concrete compressive strength, among others, and the output variable is the punching shear capacity of the slab. A dataset of 144 experimental samples was used for training and validation. To enhance the interpretability of the model, the SHapley Additive Explanations (SHAP) method was introduced to quantify the contribution of each input variable to the model's output. The results indicate that when the slab thickness exceeds 120 mm, the compressive strength is above 50 MPa, and the steel fiber volume fraction is greater than 1.0 %, the punching shear performance of SFRC slabs is significantly enhanced. In contrast, when the slab thickness is less than 80 mm, and the compressive strength is below 30 MPa, the strengthening effect of steel fibers is minimal. The proposed BPNN-GWO model achieved high prediction accuracy on the validation set, with a determination coefficient (R^2) of 0.987 and a root mean square error (RMSE) of 12.64, both of which are significantly better than those of traditional empirical models, demonstrating the applicability and superiority of the proposed method in predicting the punching shear capacity of SFRC slabs.

1. Introduction

Reinforced concrete (RC) slabs are key structural components in modern buildings. They are widely used in commercial buildings, office spaces, and residential complexes due to their high structural efficiency, low cost, and broad applicability. However, the punching shear capacity at slab–column connections often limits their overall strength. Once punching shear failure occurs, the load-bearing capacity drops sharply, potentially resulting in partial or complete structural collapse. In addition, RC slabs may experience large deflections under loading, further reducing the overall structural safety [1–3].

Studies have shown that incorporating steel fibers into concrete can effectively restrain crack propagation, improve material toughness, and enhance punching shear performance [4,5]. SFRC has gradually been introduced into slab punching design. Although current codes (e.g., ACI 318-25 [6]) have considered specific parameters of SFRC, such as correction factors for fiber volume fraction and geometry, they still rely primarily on empirical methods. A systematic design framework is lacking, especially regarding multi-parameter coupling, fiber distribution characteristics, and loading conditions. This limits the applicability and accuracy of code-based predictions for the punching shear capacity of SFRC slabs.

Previous studies have explored modeling the punching behavior of SFRC slabs. Narayanan et al. [7,8] proposed linear regression models

* Corresponding authors.
E-mail addresses: Nima.khodadadi@miami.edu (N. Khodadadi), Sax9508@163.com (A. Song).

https://doi.org/10.1016/j.rineng.2025.105646
Received 13 April 2025; Received in revised form 23 May 2025; Accepted 5 June 2025
Available online 6 June 2025

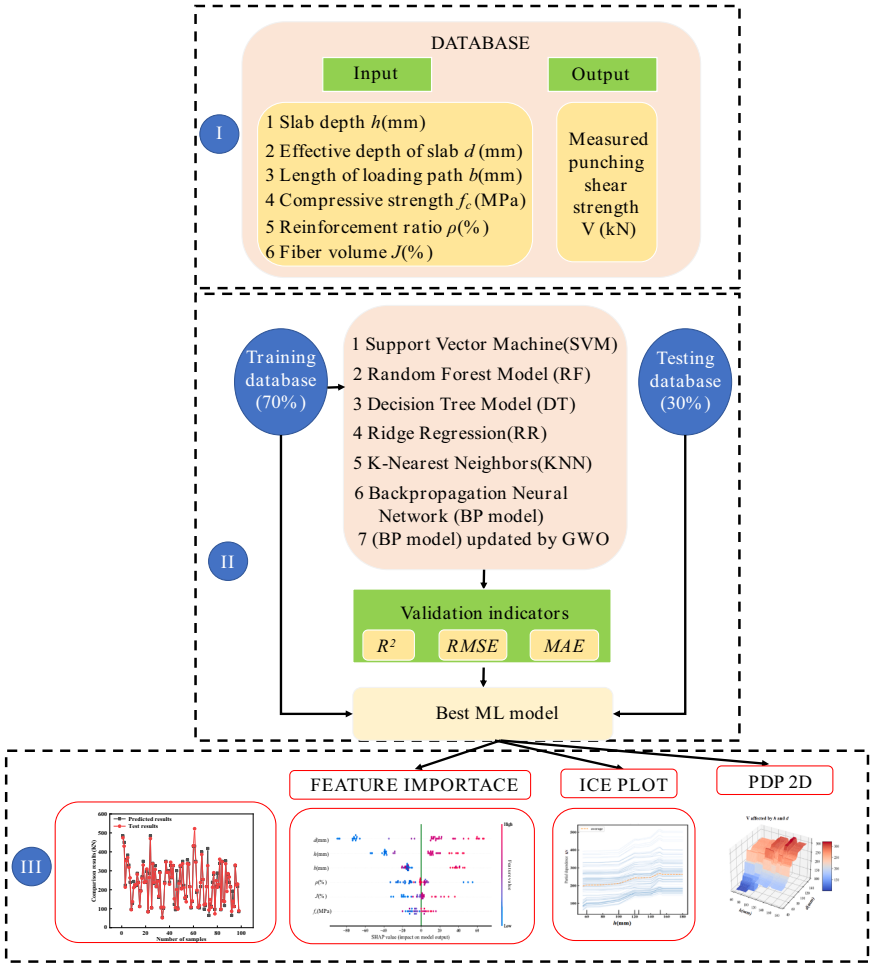

Fig. 1. Research process.

based on experimental data, using concrete compressive strength and fiber volume fraction as main variables, but the models were too simple to capture nonlinear interactions. Harajli et al. [9] systematically studied the effects of concrete strength and fiber content and found significant improvement in ultimate capacity but did not consider other parameters such as loading area. Lee et al. [10] compared different types of steel fibers and emphasized the role of fiber geometry in improving crack control and ductility. Although the proposed model was practical, it was still based on single-variable regression. Long et al. [11] used probabilistic analysis to modify traditional models, treating fiber content as a random variable, but the results were conservative and lacked adaptability. Maya et al. [12] investigated the effect of loading area size and developed a nonlinear regression model to reveal local failure patterns, but the selection of variables was still incomplete.

In summary, existing models often involve a limited number of input factors and insufficient consideration of variable interactions, resulting in restricted prediction accuracy. Therefore, it is necessary to construct a data-driven model that integrates multiple parameters, with strong expressive power and generalization ability, to reflect better the punching behavior of SFRC slabs under complex loading conditions and meet modern design requirements. There is an urgent need to develop a prediction model that can incorporate multiple influencing factors and be generalized well in order to accurately assess the punching performance of SFRC slabs and meet practical safety and design demands.

With the advancement of computational technology, machine learning (ML) has been increasingly applied in structural engineering. ML can handle large datasets and capture complex nonlinear relationships among variables, making it suitable for modeling highly complex structural performance. Previous studies, such as those by Mangalathu et al. [13] and Lu et al. [14], used artificial neural networks to predict the punching shear capacity of SFRC slabs. However, conventional ML methods often suffer from overfitting when dealing with small datasets and struggle to achieve robust generalization [15]. Metaheuristic algorithms [16] have been widely used to optimize ML models and improve performance. These algorithms have performed well in material property prediction tasks [17–19]. Among them, the Grey Wolf Optimizer (GWO) [20], as a novel algorithm, can maintain a balance between exploration and exploitation, improving model robustness and generalization in small-sample conditions [21].

This study proposes a GWO-optimized backpropagation neural network (GWO-BPNN) model to predict the punching shear capacity of SFRC slabs accurately. The model is trained using 144 experimental datasets. Input variables include slab thickness (h), effective depth (d), loading pad length (b), concrete compressive strength (f_c), reinforcement ratio (ρ), and steel fiber volume fraction (J), with hooked-end fibers having aspect ratios ranging from 50 to 80. The output variable is the slab's punching shear capacity (V). Unlike models that only consider slab thickness and concrete strength, this study introduces fiber parameters and loading area size into the input space, forming a more comprehensive feature set. SHAP results further identify sensitive intervals of key variables. These insights help guide parameter configuration and enhance the model's relevance to engineering practice. GWO is used to optimize the weights and structure of the BPNN, significantly improving the model's robustness and prediction accuracy. Finally, SHapley Additive Explanations (SHAP) are used to interpret the model output, quantify the contribution of each input variable, and reveal

interaction mechanisms, providing theoretical support for transparent modeling and structural design.

2. Research significance

Compared with existing studies, the GWO-BP neural network model proposed in this paper offers three key advantages. First, it incorporates a wider and more comprehensive influencing factors, including slab thickness, effective depth, loading pad length, concrete compressive strength, reinforcement ratio, and steel fiber volume fraction. This allows the model to reflect better the multivariable coupling relationships that influence the punching shear capacity of SFRC slabs under realistic engineering conditions. Second, the model demonstrates superior prediction accuracy. By introducing the Grey Wolf Optimizer (GWO), the model achieves stronger global parameter optimization capabilities, enabling it to more effectively capture nonlinear relationships, reduce prediction error, and enhance generalization performance. Validation results show that, compared with traditional machine learning models, the proposed model achieved the highest prediction accuracy, with an R^2 of 0.987 and an RMSE of 12.64 on the testing set. In addition, SHAP was employed to quantitatively identify each input variable's contribution and sensitivity intervals. The analysis revealed that certain variable ranges contribute most significantly to punching shear capacity enhancement. These findings provide a quantitative basis for engineering parameter selection and further improve the interpretability and practical value of the model.

3. Methodology

This section outlines the overall methodology adopted in this study. A hybrid approach was employed combining the Grey Wolf Optimization (GWO) algorithm and the Backpropagation Neural Network (BPNN). GWO was selected due to its robust global search capability and effective parameter optimization in structural prediction problems, which helps avoid local optima. As the base model, the BPNN offers a simple architecture and strong fitting capability, making it well-suited for function approximation tasks involving small to medium-sized datasets. Compared with more complex models such as Convolutional Neural Networks (CNNs), BPNNs are less dependent on large datasets and exhibit higher training efficiency.

Additionally, in contrast to Random Forest (RF) models, BPNNs are more appropriate for continuous output problems. The overall modeling framework consists of the following steps: data collection, variable partitioning, model training, testing, and SHAP analysis. The training process was conducted using 100 epochs. The dataset was randomly divided into training and testing subsets with a ratio of 70 % to 30 %. Before model training, all input features were normalized to eliminate dimensional differences and improve training effectiveness. Model performance was evaluated using standard regression metrics, including the coefficient of determination (R^2), root mean square error (RMSE), and mean absolute error (MAE). The dataset was compiled from both publicly available experimental studies and the authors' experimental results, ensuring the representativeness and diversity of the samples. Key input variables include parameters such as plate thickness and effective thickness. Six machine learning models were considered for comparison to benchmark model performance, including Support Vector Regression (SVR) and Random Forest (RF).

Furthermore, to assess the generalization capability of the proposed model, an independent dataset—distinct from the training data—was used for external validation. Finally, the SHapley Additive exPlanations (SHAP) method was employed to quantify the importance of each input variable. This interpretability analysis revealed the sensitivity intervals of key features and their nonlinear interactions, providing valuable insights for informed structural design. The overall methodological framework is illustrated in Fig. 1.

Table 1
Statistical characteristics of the variables.

Variable	h(mm)	d(mm)	b (mm)	f_c(MPa)	ρ(%)	J(%)	V(KN)
Maximum	180	154	225	65	2.53	2.2	530
Minimum	55	39	60	14	0.37	0.1	58
Average	110	86	131	37	0.99	0.71	226
Median	125	100	150	36	0.85	0.8	217
σ	33	28	46	21	0.25	0.23	110
Kurtosis	-0.83	-0.85	-1.02	-0.67	-0.36	0.03	-0.08
Skewness	-0.35	-0.29	0.31	0.10	0.80	0.23	0.60

4. Data collection

To develop a high-precision data-driven model for predicting the shear capacity of steel fiber reinforced concrete (SFRC) slabs, this study systematically collected 144 representative experimental samples from relevant literature published over the past two decades [22–36]. To ensure the consistency and applicability of the dataset, the following selection criteria were applied during the construction of the test database:

(1) Specimens must be uniaxially loaded rectangular slabs, subjected to concentrated or approximately concentrated loading to ensure a consistent shear failure mechanism;
(2) All specimens were made with ordinary Portland cement, with steel fibers uniformly distributed by being added in batches during mixing to ensure material homogeneity;
(3) Specimens were cured under standard or near-standard conditions to eliminate performance deviations caused by inconsistent curing environments;
(4) Only specimens reinforced with hooked-end steel fibers were included, with a fiber volume fraction ranging from 0.23 % to 2.2 % and aspect ratios between 50 and 80, ensuring comparability of material properties.

Table 1 summarizes the key structural parameters of the collected specimens, including slab thickness, effective depth, concrete compressive strength, reinforcement ratio, and fiber volume fraction. Fig. 2 presents the statistical distribution of these input variables. In this study, slab thickness h(mm), effective depth d(mm), slab width b(mm), concrete compressive strength f_c(MPa), reinforcement ratio ρ(%), and fiber volume fraction J (%) were selected as input variables, while shear capacity V(kN) was defined as the output variable for model development. (The blue dashed line in Fig. 2 represents the cumulative percentage of each sample.)

The data-driven modeling process consists of two stages: model construction and validation. Accordingly, the dataset was randomly divided into a training set and a testing set, with 70 % of the data (101 samples) used for model training and the remaining 30 % (43 samples) used for performance validation [32]. Data partitioning was performed using the Python platform with a random sampling strategy to ensure fair and representative distribution.

5. Research model

To ensure the computational accuracy of the model, a collinearity analysis was first conducted on the collected data to identify and eliminate highly correlated input variables. This study calculated the correlation coefficients between variables to assess the degree of multicollinearity among the inputs. Specifically, the Pearson correlation matrix was computed to evaluate the linear relationships between variables. If the absolute value of the correlation coefficient between any two variables exceeds 0.85 [35], it indicates severe multicollinearity. In such cases, the variable with less engineering significance or modeling value should be removed to reduce feature redundancy. The results of the collinearity analysis are shown in Fig. 3. It can be seen that all

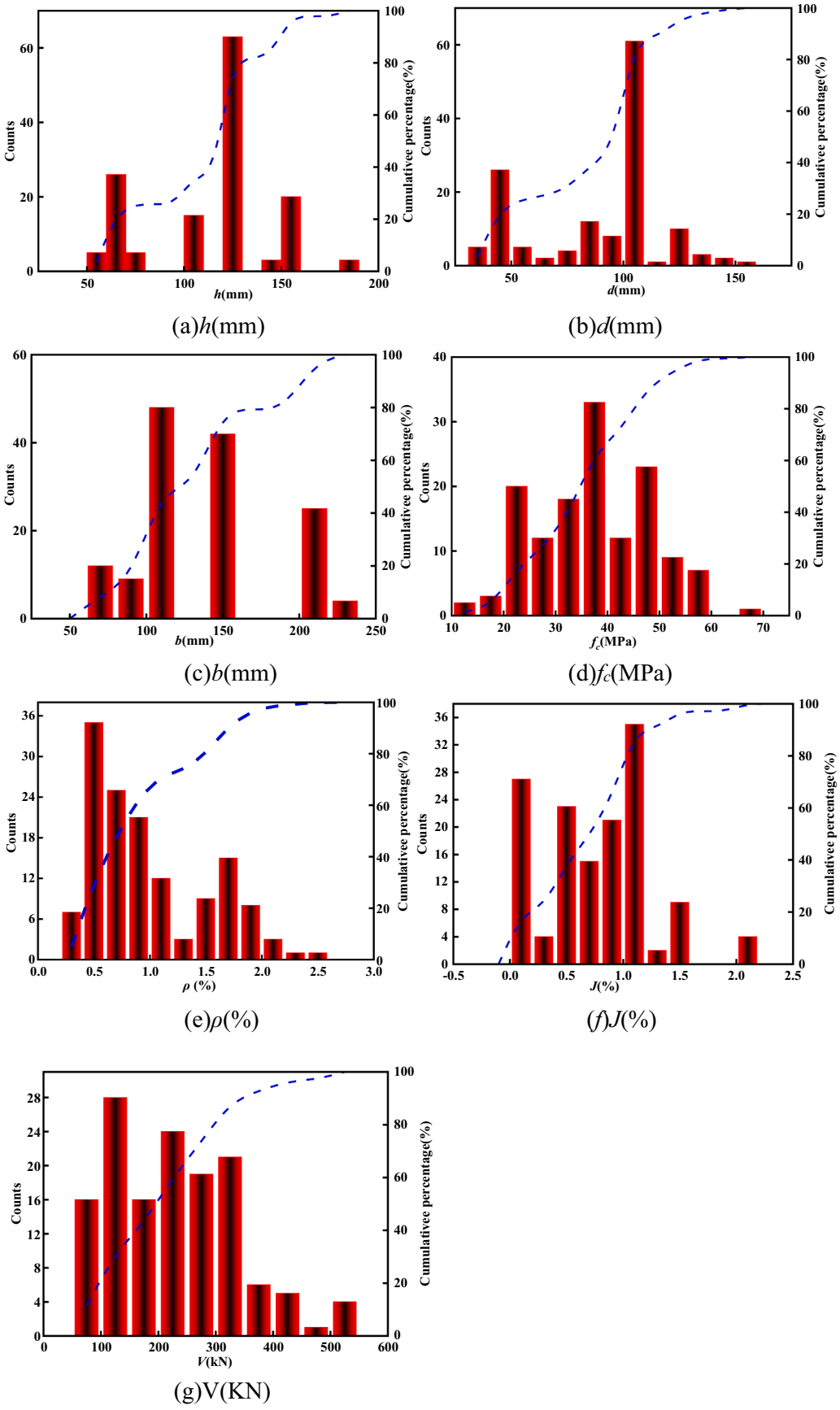

Fig. 2. Historical distributions of parameters.

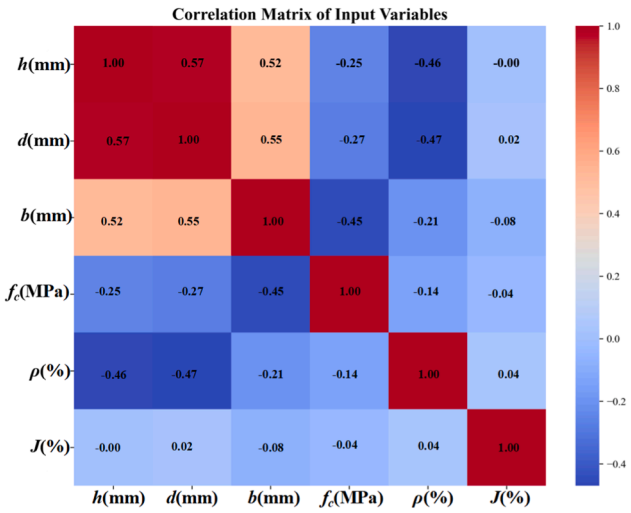

Fig. 3. Correlation matrix of input variables.

correlation coefficients are below 0.6, indicating that the selected input features exhibit a high degree of independence in physical terms and are capable of providing diverse information to support the model.

5.1. Back propagation neural network

To develop a predictive model for the shear capacity of steel fiber reinforced concrete (SFRC) slabs, this study adopts a Backpropagation (BP) neural network due to its simple structure and strong fitting capability. The model construction involves the following steps:

Step 1: *Definition of Input Layer:* The model input consists of six key parameters, forming the input vector as follows: [37].

$$x = [h, d, b, f_c, \rho, J] \tag{1}$$

Step 2: *Definition of Hidden Layer*: The network architecture adopts a single hidden layer with 10 neurons to fully capture the nonlinear relationships among input features while maintaining model simplicity. The hidden layer utilizes the ReLU (Rectified Linear Unit) activation function, which offers advantages such as fast convergence and stable gradients in regression tasks, effectively mitigating the vanishing gradient problem. Compared to traditional activation functions like Sigmoid and Tanh, ReLU demonstrates superior training efficiency and predictive performance on the dataset used in this study, as shown in Eq. (2). To further enhance model performance, grid search is employed to systematically optimize key hyperparameters, including the learning rate, number of training epochs, and batch size, ensuring robust model convergence and generalization capability. The forward propagation process of the hidden layer is presented in Eq. (3) [37].

$$f(x) = \max(0, x) \tag{2}$$

In this case, $f(x)$ is the output parameter.

$$Z_j = \sum_{i=1}^{n} w_{ij} x + b_j \tag{3}$$

Where w_{ij} is the input weight, x is the input feature, and b_j represents the bias term. The bias term shifts the activation output, boosting model flexibility and preventing neuron saturation [38].

Step 3: *Definition of Output Layer*: The output layer is the final layer of the neural network, which directly generates the network's final output. The task of the output layer is to convert the processed results from the last hidden layer into the final output that can be used for classification, regression, or other tasks. The process includes the following steps: calculating the error of the output layer, back-propagating the error to the hidden layers, updating the weights and biases, and gradually converging to the predicted result. Typically, metrics such as the residual between the predicted and actual values are used to evaluate the error of the output layer. The error is then propagated back to the hidden layers. For each neuron i in hidden layer l, the error is calculated using the formula shown in Eq (4) [39].

$$\delta_i^l = \left(\sum_j \delta_j^{l+1} \times w_{ij}^{l+1} \right) \times \sigma(z_i^l) \tag{4}$$

Where δ_i^l represents the error of neuron i in hidden layer l, δ_i^{l+1} denotes the error value of neuron j in the next layer, w_{ij}^{l+1} is the weight from neuron i in hidden layer l to neuron j in the next layer l+1, and $\sigma(z_i^l)$ is the derivative of the activation function of neuron i in hidden layer l. The weights and biases are updated by using the error calculated through backpropagation. The gradient descent optimization algorithm is applied to update the weights and biases, and the specific update process is shown in Eq. (5) [39].

$$\begin{aligned} w_{ij}^l &\leftarrow \eta \times \delta_j^{l+1} \times a_i^l \\ b_j^{l+1} &\leftarrow \eta \times \delta_j^{l+1} \end{aligned} \tag{5}$$

Where η represents the learning rate, b_j^{l+1} denotes the bias of neuron j in hidden layer l+1, and a_i^l is the activation value of neuron i in hidden layer l.

5.2. Gray wolf algorithm

The BP model is prone to getting trapped in local optima and often encounters issues such as overfitting or underfitting, adversely affecting model accuracy. The Grey Wolf Optimizer (GWO), inspired by the social hierarchy and hunting behavior of grey wolves, possesses global exploration and local exploitation capabilities. Compared to other metaheuristic algorithms like Adam [40], Particle Swarm Optimization (PSO) [41], and Genetic Algorithm (GA), GWO demonstrates superior convergence speed and predictive accuracy in this study. It can be utilized to optimize the weights and biases of the BP neural network, thereby addressing these issues. The specific steps are as follows [39]:

$$f(w) = Loss(BP_{network}(w)) \tag{6}$$

Where: w represents the neural network weights, and Loss denotes the loss function. Based on the performance of each wolf, their positions are adjusted. By simulating the hunting behavior of grey wolves, their positions are updated to gradually approach the optimal solution of the model. The update process is shown in Eq. (7) [42].

$$X_i(t+1) = X_i(t) + A_i \times (X_{best} - C_i \times X_{best} - X_i(t)) \tag{7}$$

Where $X_i(t)$ represents the position of the *i-th* wolf during the *t*-th iteration, X_{best} is the position of the current optimal solution, and A_i and C_i are random coefficients that control the magnitude of the wolf's position update. During the position update process, the neural network's loss function value corresponding to each wolf's new position is calculated to evaluate its fitness, and the wolf with the best fitness is selected as the current optimal solution. The above steps are repeated until the stopping condition is met (e.g., reaching the maximum number of iterations or the fitness satisfying a threshold).

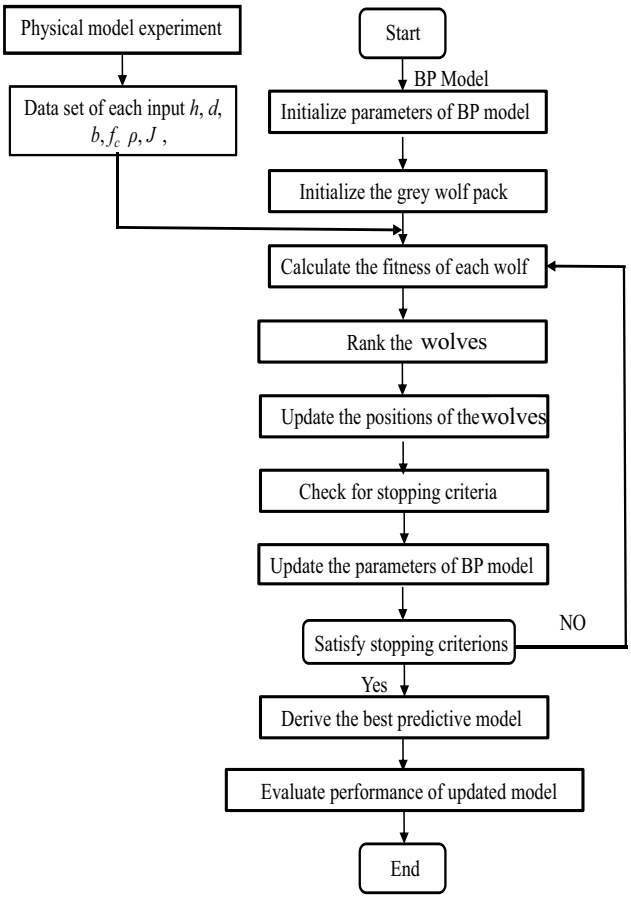

Fig. 4. Calculation process of the BP model improved by GWO.

It is worth noting that this paper does not directly adopt the standard form of GWO but instead combines engineering prior knowledge to constrain the initialization of the search space, thereby improving search efficiency. Comparative results show that, compared to the Adam optimizer, GWO reduces model training time by approximately 35 % and decreases the test set MSE error by 12.6 %, demonstrating significant performance improvements. Fig. 4 illustrates the computational steps of the neural network model improved by the GWO.

6. Results

6.1. Performance evaluation of GWO-BP model

The entire modeling process was carried out using Python. According to previous studies [43], the BP neural network was designed with a single hidden layer containing 10 neurons, balancing computational efficiency and prediction accuracy. To enhance the performance of the BP network, the Grey Wolf Optimizer (GWO) was used to fine-tune the model's weights and biases. Several key parameters within the GWO algorithm significantly impact the optimization outcome, including the population size, social hierarchy structure, convergence factor, and the maximum number of iterations. The population size determines how broadly the solution space is explored. A larger population allows for better exploration and helps the algorithm avoid getting stuck in local minima, though it also increases computation time. For relatively low-dimensional or straightforward problems, a population size between 10 and 30 is often sufficient [43]. In contrast, more complex or high-dimensional problems typically require a population of 50 to 100 wolves [43]. The social hierarchy in GWO consists of three primary roles: α, β, and δ. α represents the position of the leading wolf, followed by β and δ. During optimization, these lead wolves guide the rest of the pack (other candidate solutions). The movement and decision-making of the wolves are influenced by two key vectors: the weight vector (A) and the convergence factor (C). The weight vector A governs how far a wolf moves toward or away from a leader, evolving over time to balance exploration and exploitation. It's calculated as $A = 2 \times R_1 - 1$, where R_1 is a random number between 0 and 1. The value of A generally fluctuates between -2 and 2. Larger absolute values of A encourage global exploration, while smaller values promote local refinement. The convergence factor C helps guide the wolves toward the target (i.e., the best solution) and typically ranges from 0 to 2. The value of C is calculated as $2 \times R_2$ [43], where R_2 is also a random number between [0, 1]. The larger the value of C, the stronger the wolves' tendency to follow the leader, enhancing the ability to exploit the current optimal solution.

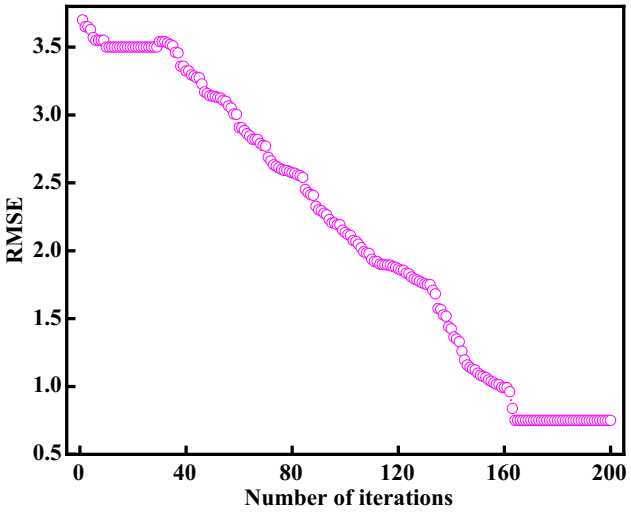

Fig. 5. Variations in RMSE throughout the iterative update process.

Considering the highly nonlinear and complex relationship between the input and output variables, the maximum number of iterations for the model was set to 200. The Root Mean Square Error (*RMSE*) was used to evaluate the model's prediction accuracy under different iteration counts. The calculation method is as follows [43]:

$$RMSE = \sqrt{\frac{1}{n}\sum_{i=1}^{n}(y - y')^2} \tag{8}$$

Where y represents the measured results, y' denotes the predicted results, and n is the number of samples. The variation trend of *RMSE* values during the training process is illustrated in Fig. 5. The results indicate that after 160 iterations, the RMSE stabilizes at approximately 0.75, suggesting that the model has reached its optimal state. Furthermore,

Fig. 6 displays the predicted punching shear capacity of SFRC slabs. These graphs provide a comparative analysis of the training and validation dataset's measured and predicted bearing strengths (V). The results demonstrate that the BP neural network model optimized by the grey wolf algorithm can predict the punching shear capacity of SFRC slabs under various conditions with reasonable accuracy. Although some discrepancies exist at extreme values of punching shear capacity, the optimized BP neural network model accurately captures the variation trend of SFRC slab punching shear capacity, underscoring its potential value in predicting the punching shear capacity of SFRC slabs in different scenarios. Reasons for discrepancies at extreme points:(1) Few training samples in the extreme value range lead to insufficient model learning. (2) Structural behavior is more complex and nonlinear under extreme punching shear capacity. (3) Key structural parameters have a greater impact at extreme points, increasing prediction difficulty.

To further validate the model's generalization capability, 20 data sets were collected from other literature sources [44,45]. These 20

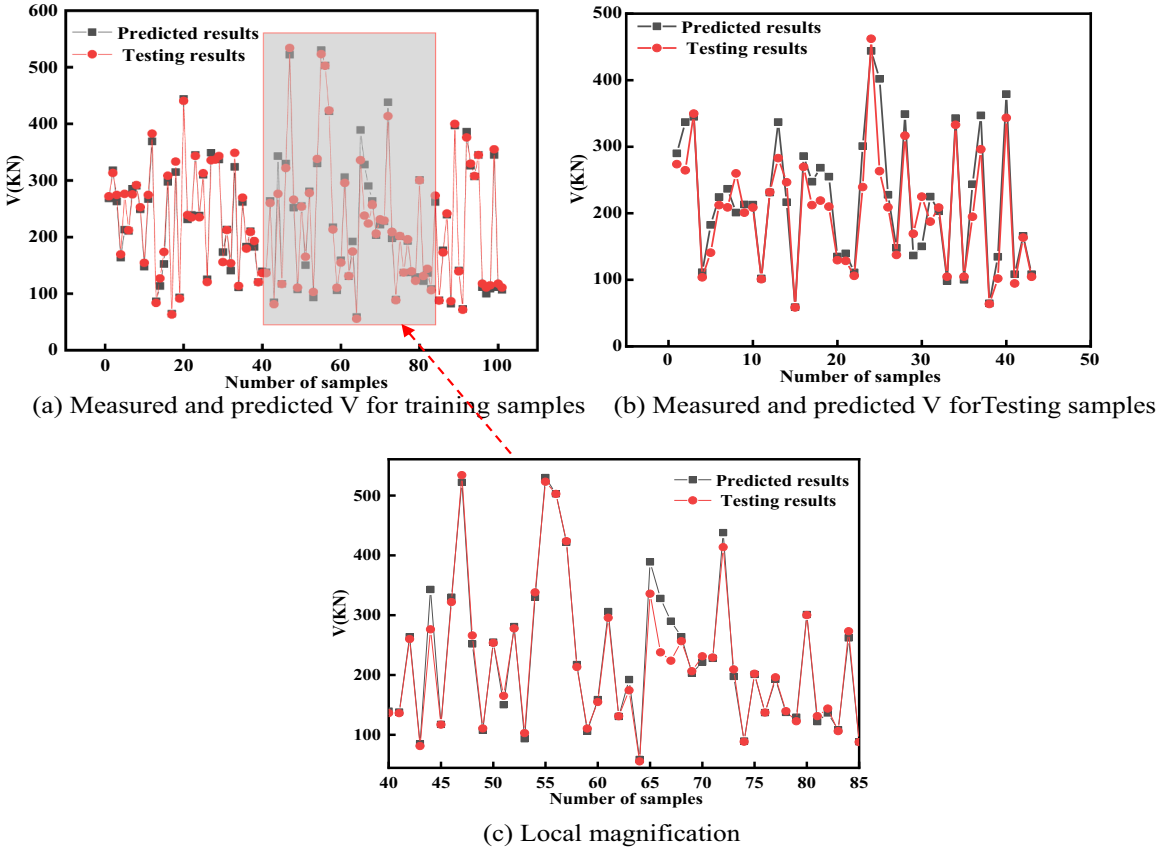

Fig. 6. Comparison results between predicted and test.

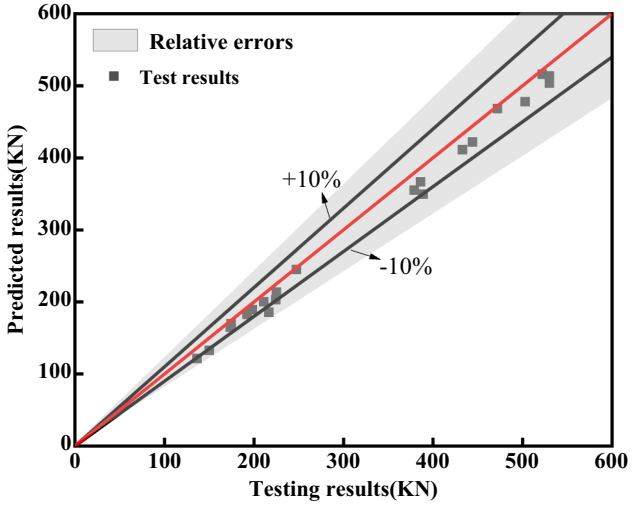

Fig. 7. Comparative results of the punching shear capacity of SFRC slabs.

datasets cover different structural types and design parameters, all sourced from relevant experimental studies. They specifically include variations in reinforcement ratios, concrete strength grades, and geometric dimensions of the components, with value ranges consistent with those in Section 4. All data have undergone the same preprocessing procedures as the training set to ensure fairness and consistency in model validation. Following the procedures outlined in Section 6.1, the punching shear capacity of SFRC slabs was predicted, with the results presented in Fig. 7. The findings indicate that the predicted results closely align with the measured values, with the relative error for most samples falling within 10 %. This demonstrates that the model exhibits high accuracy and reliability.

6.2. *Benchmark comparison of typical machine learning model*

To further assess the prediction accuracy of the proposed model, six widely used machine learning algorithms were selected for comparison. These include Random Forest (RF), Support Vector Machine (SVM), Decision Tree (DT), Ridge Regression (RR), K-Nearest Neighbors (KNN), and the standard BP Neural Network [46]. All models were trained and tested using the same input and output variables detailed in Section 4 to ensure consistency in the evaluation. Among these, the SVM model is commonly used for both classification and regression tasks. Its core objective is to identify an optimal hyperplane that best separates data points, maximizing the margin between different categories. To enhance prediction performance across all models, the input data were first normalized—ensuring the models operated on a consistent scale and reducing the influence of variable magnitudes.

In addition, due to the complex and nonlinear relationship between the input and output variables, the Radial Basis Function (RBF) kernel was selected for the SVM model to better handle nonlinear patterns in the data [47]. The Random Forest (RF) model operates as an ensemble method comprising multiple decision trees. The number of trees in the forest was set to 100, the maximum depth of the trees was set to 10, and the minimum number of samples required to split an internal node was set to 5 [48]. The basic parameters of the DT model were set to match those of the RF model. Ridge Regression, also known as Tikhonov regularization, is an improved linear regression version. Adding a regularization term to the loss function controls model complexity and prevents overfitting. KNN is a non-parametric and lazy learning algorithm. It works by identifying the K nearest neighbors to a new data point in a pre-labeled dataset and predicting the label of the new data

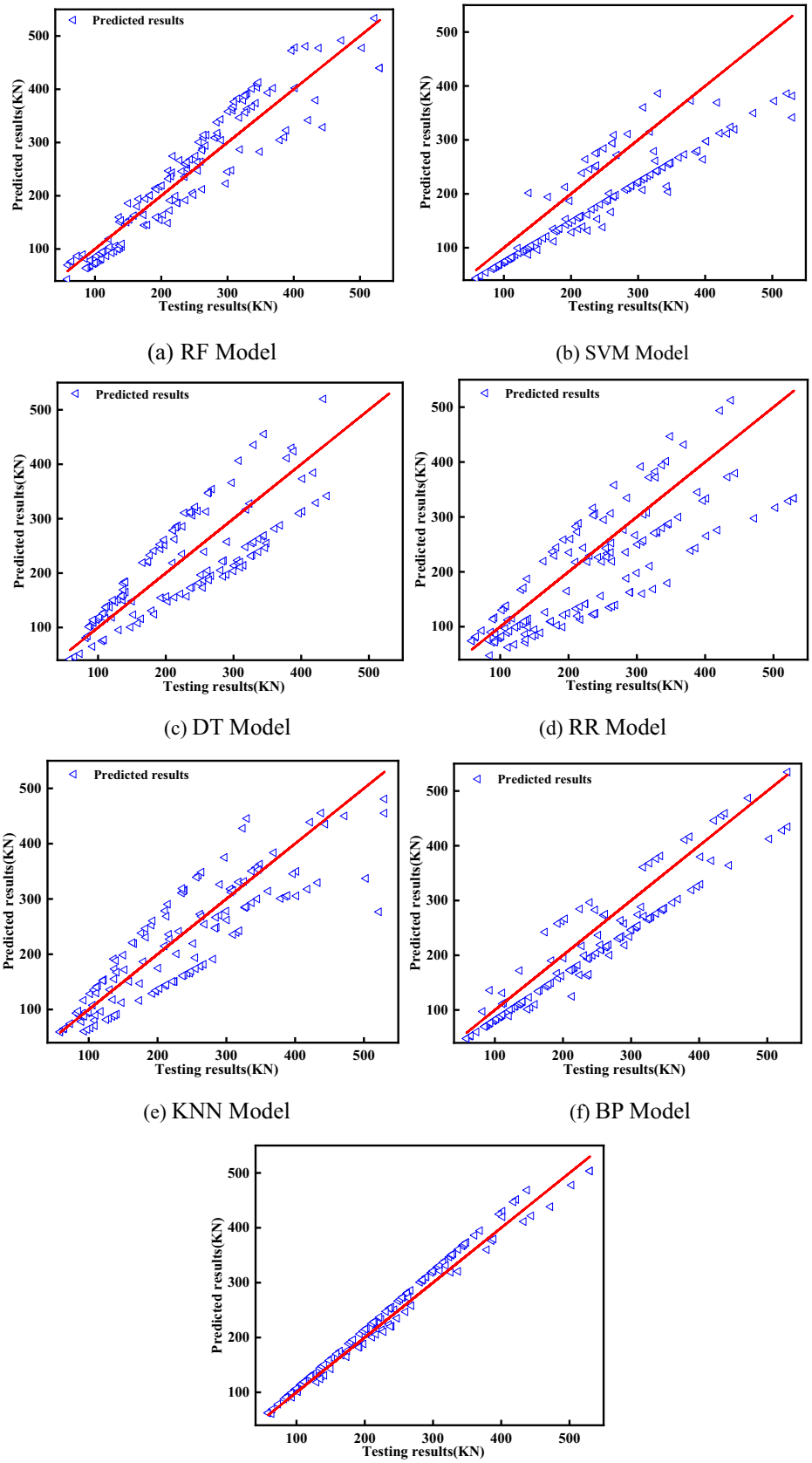

(a) RF Model (b) SVM Model

(c) DT Model (d) RR Model

(e) KNN Model (f) BP Model

(g) BP Model updated by GWO

Fig. 8. Evaluation results of typical machine learning model.

Table 2
Formulation of each evaluation metric.

Performance Metric	Expression
RMSE (Root Mean Square Error)	$RMSE = \sqrt{\frac{1}{n}\sum_{i=1}^{n}(y-y')^2}$
MAE (Mean Absolute Error)	$MAE = \frac{1}{n}\sum_{i=1}^{n}\lvert y-y'\rvert$
R^2 (Coefficient of Determination)	$R^2 = 1-\frac{\sum_{i=1}^{n}(y-y')^2}{\sum_{i=1}^{n}(y-\bar{y})^2}$
MAPE (Mean Absolute Percentage Error)	$MAPE = \frac{1}{n}\sum_{i=1}^{n}\left\lvert\frac{y-y'}{y}\right\rvert$
RAE (Relative Absolute Error)	$RAE = \frac{1}{n}\sum_{i=1}^{n}\left\lvert\frac{y-y'}{y-\bar{y}}\right\rvert$
MSE (Mean Squared Error)	$MSE = \frac{1}{n}\sum_{i=1}^{n}(y-y')^2$

Table 3
Evaluation results of each model.

Model name	RMSE	MAE	R^2	MAPE	RAE	MSE
RF	24.08	17.84	0.857	6.64	0.21	724.8
SVM	38.96	29.92	0.815	10.72	0.34	1898.16
DT	32.41	25.68	0.83	8.88	0.29	1312.24
RR	44.16	34.08	0.782	11.68	0.38	2437.44
KNN	36.48	26.8	0.841	9.6	0.31	1664.24
BP	20.24	14.96	0.912	5.2	0.17	512.08
GWO-BP	12.64	7.76	0.987	2.72	0.09	199.68

point based on the majority label of these neighbors. The accuracy of the KNN model is influenced by the value of K. A smaller K value makes the model more sensitive to the training data, which may lead to overfitting.

In comparison, a more considerable K value increases computational cost and may prevent the model from capturing the general characteristics of the data, resulting in underfitting. Cross-validation analysis revealed that the highest prediction accuracy was achieved when $K=5$ [49]. The parameters for the BP neural network were set following the steps outlined in Section 6.1. The prediction results of all the models following these steps are shown in Fig. 8.

Fig. 8 presents the prediction results of various machine learning models for the punching shear capacity of SFRC slabs. The blue points represent the predicted values from each model, while the red line denotes the ideal fit line ($y=x$), representing a perfectly accurate prediction. The closer the data points are to this line, the higher the model's prediction accuracy. The results indicate that the BP neural network model improved through the grey wolf optimization algorithm and performed the best, with minimal error between the predicted and measured values. This suggests that the model effectively captures the complex nonlinear relationships between the input and output variables. Following closely behind are the BP neural network without grey wolf optimization and the RF model, which also exhibited high prediction accuracy, albeit slightly inferior to the improved BP neural network.

Six different evaluation metrics were selected (as shown in Table 2) for quantitative assessment to further evaluate each model's prediction accuracy. The performance of the models under these metrics is summarized in Table 3.

Table 3 presents the evaluation results of seven different models for the prediction task. Overall, the GWO-BP model delivers the best performance, achieving the lowest values in all error metrics (e.g., RMSE of 12.64 and MAE of 7.76) and the highest coefficient of determination (R^2=0.987), indicating excellent prediction accuracy and strong fitting capability. In contrast, the traditional RR model performs the worst, with the lowest R^2value (0.782) and the highest error across the board, suggesting it is less suitable for this task. The BP and RF models also show relatively good performance, with R^2values of 0.912 and 0.857, respectively, making them viable options where high prediction accuracy is required. Overall, among the models considered in this study, the GWO-optimized BP neural network achieved the best performance.

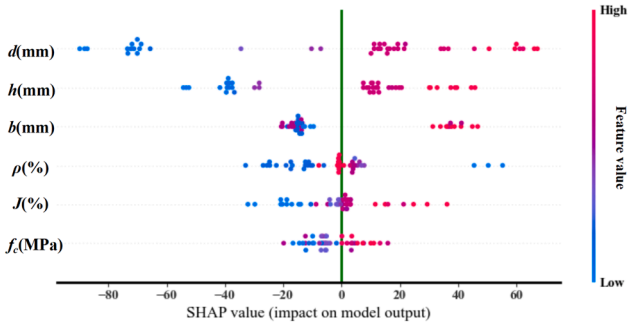

Fig. 9. Analysis results of the importance of each input variable.

7. Discussion

This section analyzes the impact of each input variable on the predicted punching shear capacity of SFRC slabs, clearly revealing the contribution of each factor to the model's output and ranking their relative importance in the prediction process. By adjusting individual input variables one at a time, the local response of the model to changes in each variable was explored. The interactions between different input variables were examined, illustrating how variable interdependencies influence the model's behavior.

7.1. Feature Importance

In this study, the SHapley Additive Explanations (SHAP) method [50] was used to analyze the contribution of each input variable to the punching shear capacity of SFRC slabs. SHAP values offer two key insights: (1) the degree to which each input variable influences the model's predicted output, as reflected by the spread along the y-axis, and (2) how the actual values of these input variables affect the prediction, shown by the distribution along the x-axis and the color of the data points. Red points represent higher feature values, which generally have a positive impact on the prediction, while blue points indicate lower feature values, typically associated with a negative effect. The analysis results are shown in Fig. 9.

The results indicate that slab thickness (h) and steel fiber volume fraction (J) have the most significant positive impact on the model output. This is because both variables directly enhance the shear performance of the slab under loading. Specifically, increasing the slab thickness enlarges the cross-sectional area of the member, which expands the potential punching shear failure surface, thereby significantly improving shear capacity. The addition of steel fibers enhances the toughness of the concrete, helps control the development and propagation of cracks, enhances the material's post-peak behavior and failure mode, and ultimately delays the onset of punching failure. Loading pad length (b) and reinforcement ratio (ρ) also show a certain degree of positive influence. As seen in the SHAP plot, higher values of these variables (in red) are associated with positive SHAP values, indicating a favorable impact on punching shear capacity. A larger loading pad helps to spread out the applied load, reducing stress concentrations and improving the local shear performance.

Meanwhile, a higher reinforcement ratio improves the synergy between steel and concrete, increasing both ductility and shear resistance in the post-cracking phase. Although concrete compressive strength (f_c) and effective depth (d) have relatively smaller impacts, their higher values still contribute positively to the model's output. Higher compressive strength provides better inherent shear resistance within the concrete matrix, while increased effective depth improves the internal lever arm of the reinforcing steel, indirectly enhancing the slab's shear capacity.

Overall, the behavior of each input variable in the model aligns well with theoretical expectations and engineering practice. The model's

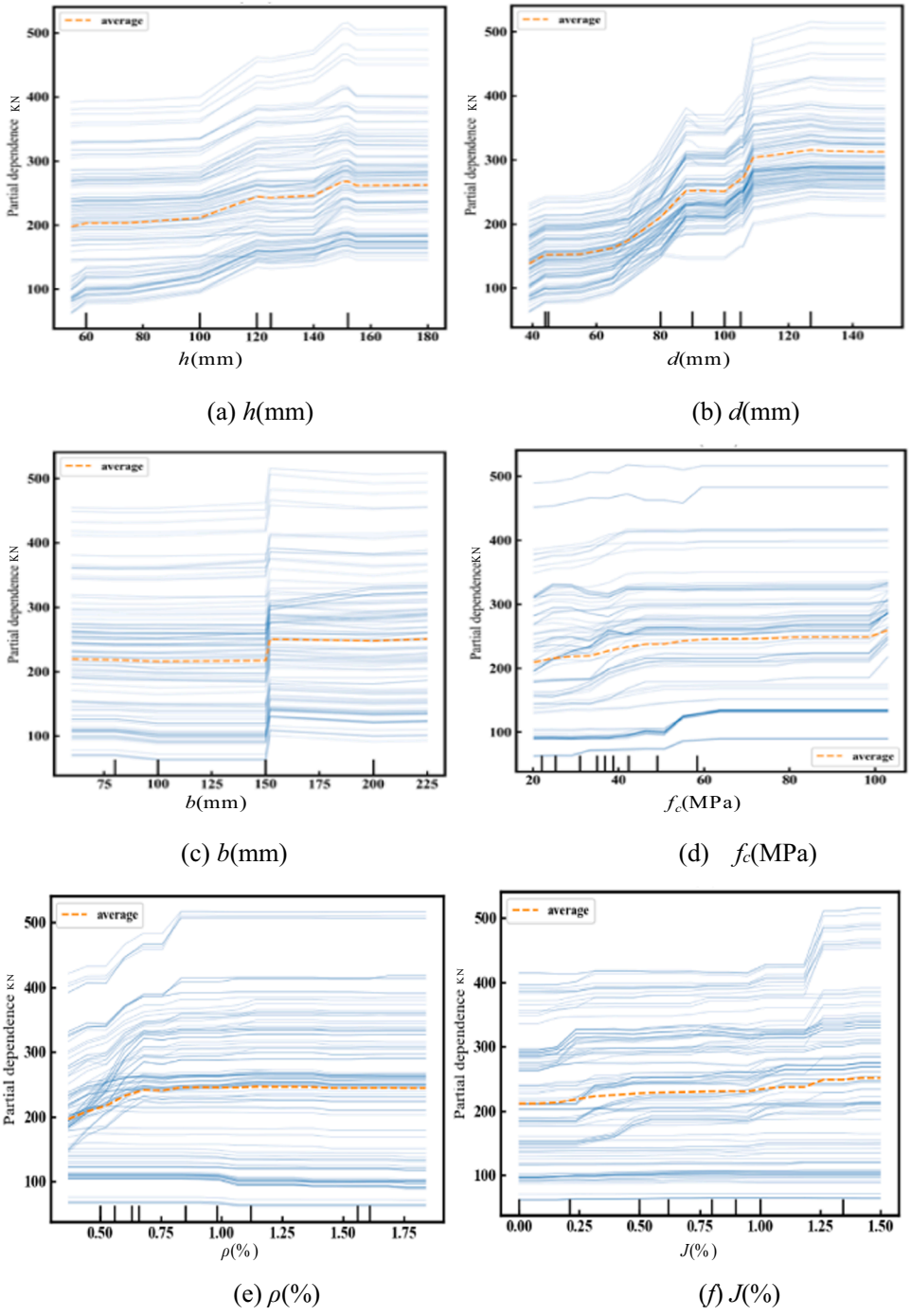

(a) h(mm) (b) d(mm)

(c) b(mm) (d) f_c(MPa)

(e) ρ(%) (f) J(%)

Fig. 10. Individual conditional expectation analysis of input variables.

predictions closely match the actual data in the database, and the SHAP analysis provides clear and interpretable insights into the contribution of each variable, validating the model's reliability and practical applicability. However, some limitations remain. First, the attribution provided by SHAP depends on the distribution of the training data, and in sparse regions of the feature space, the explanations may carry a certain degree of uncertainty and risk of misinterpretation. Additionally, different train/test splits may result in some variation in SHAP values. Although consistent attribution trends were observed across multiple random splits, cross-validation of SHAP results is still recommended for practical use.

Furthermore, although this study also employed ICE (Individual Conditional Expectation) and PDP (Partial Dependence Plot) methods to supplement the analysis of marginal effects, their generalizability in regions with strong feature interactions or low sample density remains to be verified. Future research should consider integrating more robust interpretability techniques and uncertainty quantification methods to enhance the stability and credibility of model explanations.

7.2. Analysis of individual conditional expectations and partial dependencies

Fig. 10 shows the Individual Conditional Expectation (ICE) trends for each input variable, revealing the specific influence mechanisms of variables on the punching shear capacity of SFRC slabs at different stages. For example, when the slab thickness increases from 60 mm to

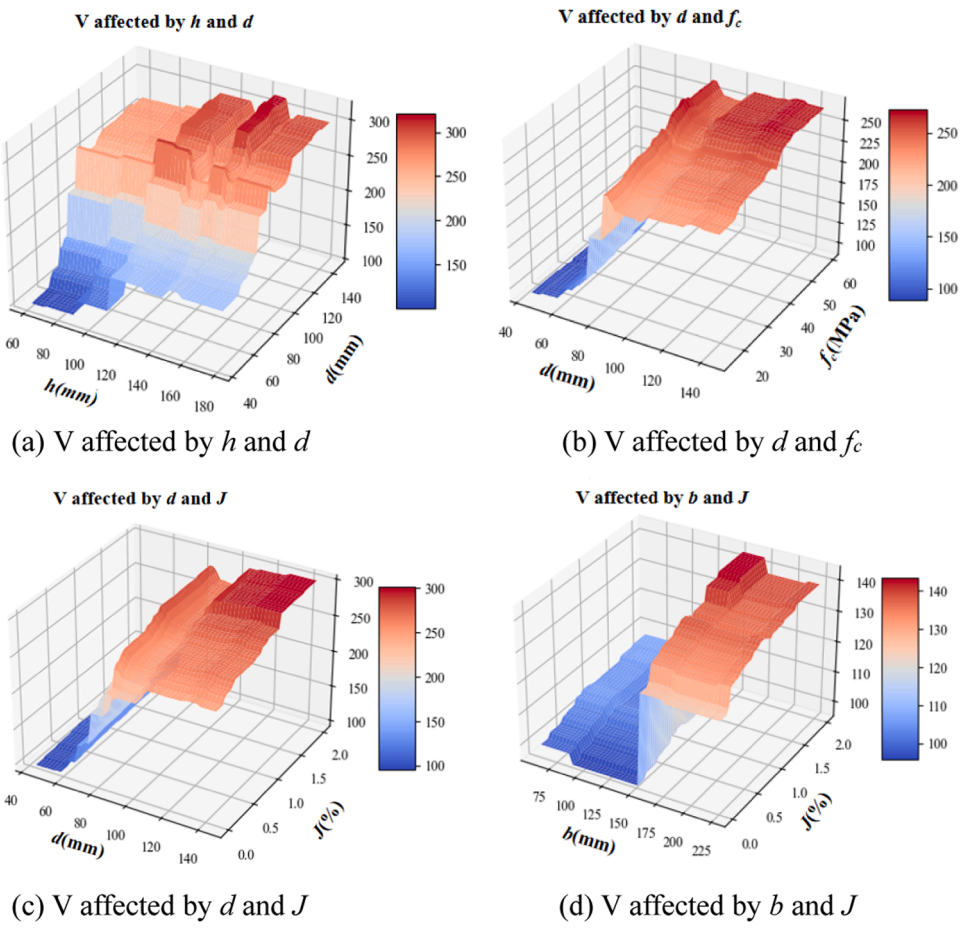

Fig. 11. Interaction between input variables and output variables.

180 mm, the punching shear capacity significantly improves, especially after surpassing 100 mm. This is mainly because thicker slabs can more effectively distribute and bear punching shear forces, reducing stress concentration and thereby significantly enhancing the shear resistance of the structure. The reinforcement ratio also substantially enhances the shear capacity within the 0.5 % to 1.5 % range, with the effect peaking near 1.5 %. This indicates that proper steel reinforcement improves the ductility and load-bearing capacity of the structure, preventing brittle failure. Although fiber volume overall improves shear capacity, its impact is limited at lower contents, likely because fibers at low volume fractions do not form a sufficient three-dimensional reinforcing network to inhibit crack propagation effectively. The increase in compressive strength, especially from 20 MPa to 60 MPa, significantly boosts the shear capacity. This is primarily due to the enhanced concrete strength improving the overall structural capacity and crack resistance, reducing the initiation and propagation of microcracks. In contrast, the influence of loading pad length is smaller. It tends to stabilize, indicating that beyond a specific size, enlarging the loading area has a limited effect on optimizing stress distribution and cannot significantly improve punching shear performance.

Fig. 11 provides a detailed view of the interactions between variables and their combined effect on punching shear capacity through two-dimensional partial dependence plots. The combined increase in slab thickness and effective depth notably enhances the capacity, with a marked rise after the thresholds of 120 mm and 100 mm, respectively. This reflects that optimizing structural geometry can improve the section's resistance to punching shear failure. The synergy between effective depth and compressive strength demonstrates the joint effect of material properties and structural dimensions; when both increase, the strength enhancement better leverages the geometric advantages of the structure. The combination of effective depth and fiber volume shows a steadily increasing trend, suggesting that fiber-reinforced concrete plays a more significant role in thicker slabs by effectively inhibiting crack propagation and enhancing structural toughness. The joint effect of loading pad length and reinforcement ratio reveals that reasonable load distribution and steel reinforcement configuration can collaboratively improve load-bearing capacity and prevent premature failure caused by local stress concentrations.

In summary, Figs 10 and 11 reflect the influence trends of various variables on the punching shear capacity of SFRC slabs and reveal the underlying structural mechanics and material performance mechanisms behind these effects, providing strong support for theoretical analysis and engineering design.

8. Conclusion

Accurately characterizing the punching shear capacity of steel fiber reinforced concrete (SFRC) slabs is challenging due to the complex, nonlinear interactions among multiple influencing factors. Traditional predictive models often fail to capture these interactions effectively, particularly under varying structural and material conditions. In this study, we developed a hybrid prediction model by integrating the Grey Wolf Optimizer (GWO) with a backpropagation neural network (BP) to improve prediction accuracy and model generalization. The SHAP (SHapley Additive exPlanations) method was further employed to interpret variable contributions and identify sensitivity intervals, offering insights into the design relevance of input parameters. The key findings and contributions of this study are as follows:

- **Improved prediction performance:** The proposed GWO-BP neural network outperforms conventional machine learning models in predicting the punching shear capacity of SFRC slabs. It achieved a coefficient of determination (R^2) of 0.987 and a root mean square error (RMSE) of 12.64 on the test set. Most predictions fell within a 10 % relative error range of the experimental data, demonstrating both accuracy and generalization capability.
- **Quantified variable contributions:** The SHAP-based interpretability analysis revealed that slab thickness and fiber volume fraction are the most influential variables. Increased slab thickness (>120 mm) and fiber content (>1.0 %) significantly enhance punching shear performance. Loading pad length and reinforcement ratio also play notable roles by improving load distribution and ductility. Although effective depth and compressive strength had relatively smaller effects, they contributed positively to shear resistance.
- **Identification of sensitivity intervals:** Partial dependence analysis showed that punching shear capacity improves markedly when key parameters exceed certain thresholds: slab thickness above 120 mm, effective depth above 100 mm, compressive strength above 50 MPa, and fiber volume fraction exceeding 1.0 %. Conversely, when parameters fall below critical levels (e.g., thickness <80 mm or strength <30 MPa), the improvement in capacity is limited.
- **Limitations and future work:** While the model demonstrates strong performance, it is trained on a limited size and scope dataset. Its generalizability may be affected by variable distributions and unconsidered factors such as environmental degradation, fatigue, or long-term loading effects. Future studies should incorporate broader datasets and consider deploying the model in practical design platforms. In addition, further exploration of advanced hybrid algorithms and their integration into code-based design frameworks is warranted.

Ethical approval

This article does not contain any studies with human participants or animals performed by any of the authors. Informed consent was not required as no human or animals were involved.

CRediT authorship contribution statement

XuanRui Yu: Writing – original draft, Visualization, Methodology, Conceptualization. **Nima Khodadadi:** Writing – original draft, Visualization, Software, Methodology, Investigation. **Anxiang Song:** Writing – original draft, Visualization, Formal analysis, Data curation, Conceptualization. **Yang Yu:** Writing – original draft, Methodology, Conceptualization. **Antonio Nanni:** Writing – review & editing, Supervision, Resources.

Declaration of competing interest

The authors declare that they have no known competing financial interests or personal relationships that could have appeared to influence the work reported in this paper.

Acknowledgements

This work is supported by the Chongqing University of Science and Technology Research Funding Project (ckrc20240616) and the financial support from the National Science Foundation I/U-CRC Center for Integration of Composites into Infrastructure (CICI) under grant 1916342.

Data availability

Data will be made available on request.

References

[1] X. Wu, X.L. Fan, Z.Y. Xie, M.M. Sun, H.M. Qian, C.Q. Wang, Experimental study on punching performance of concrete slab reinforced with GFRP grids, Structures 76 (2025) 108974.
[2] N. Oukaili, I. Peera, Predictive model for stress at ultimate in internally unbonded steel tendons based on genetic expression programming, Results. Eng. 13 (2022) 100386.
[3] A. Alateyat, R. Awad, B. Ibrahim, M.T. Junaid, S. Altoubat, M. Maalej, S. Barakat, Punching shear strength of fiber-reinforced polymer concrete slabs: database-driven assessment of parameters and prediction models, Eng. Struct. 315 (2024) 118511.
[4] J A Mcmahon, A C Birely, Service performance of steel fiber reinforced concrete (SFRC) slabs [J], Eng. Struct. (08) (2018) 58–68.
[5] Alireza, Gholamhoseini, Amir, An experimental study on strength and serviceability of reinforced and steel fibre reinforced concrete (SFRC) continuous composite slabs [J], Eng. Struct. (05) (2016) 171–180.
[6] ACI, ACI Committee 318, Building code requirements for structural concrete (ACI 318–011) and commentary (ACI 318R–11), American Concrete Institute, Farmington Hills (MI), 2011.
[7] R. Narayanan, I Y S Darwish, Punching shear tests on steel-fibre-reinforced microconcrete slabs, Mag. Concr. Res. 39 (1987) 42–50.
[8] M Y Cheng, G J Parra-Montesinos, Evaluation of steel Fiber reinforcement for punching shear resistance in slab-column connections-part I: monotonically increased load, Struct. J. 107 (2010) 101–109.
[9] M H Harajli, D. Maalouf, H. Khatib, Effect of fibers on the punching shear strength of slab-column connections, Cem. Concr. Compos. 17 (1995) 161–170.
[10] J H Lee, Y S Yoon, W D Cook, et al., Improving punching shear behavior of glass Fiber-reinforced polymer reinforced slabs, ACI. Mater. J. (4) (2009) 106.
[11] M. LongN, R. Mariain, T.Q. Toan, Punching shear capacity of lnterior SFRC slab-column connections, J. Struct. Eng. (08) (2011) 22–37.
[12] L F Maya, M F Ruiz, A. Muttoni, et al., Punching shear strength of steel fibre reinforced concrete slabs, Eng. Struct. (07) (2012) 83–94.
[13] S. Mangalathu, H. Shin, E. Choi, Explainable machine learning models for punching shear strength estimation of flat slabs without transverse reinforcement, J. Build. Eng. (2) (2021) 102300.
[14] S. Lu, M. Koopialipoor, P G Asteris, et al., A novel feature selection approach based on tree models for evaluating the punching shear capacity of steel Fiber-reinforced concrete flat slabs, Materials (13) (2020) 10–23.
[15] J. Yan, J. Su, J. Xu, Explainable machine learning models for punching shear capacity of FRP bar reinforced concrete flat slab without shear reinforcement [J], Case Stud. Constr. Mater. (20) (2024) 20–32.
[16] A. Kaveh, S. Talatahari, N. Khodadadi, Stochastic paint optimizer: theory and application in civil engineering, Eng. Comput. (2022) 1–32.
[17] N. Oukaili, I. Peera, Stress at ultimate in internally unbonded steel based on genetic expression programming [J], ACI. Struct. J. 119 (6) (2022) 177–191.
[18] N. Khodadadi, H. Roghani, E. Harati, M. Mirdarsoltany, F. De Caso, A. Nanni, Fiber-reinforced polymer (FRP) in concrete: a comprehensive survey, Constr. Build. Mater. 432 (2024) 136634.
[19] N. Khodadadi, H. Roghani, F. De Caso, E.S.M. El-kenawy, Y. Yesha, A. Nanni, Data-driven PSO-CatBoost machine learning model to predict the compressive strength of CFRP-confined circular concrete specimens, Thin-walled Struct. 198 (2024) 111763.
[20] S. Mirjalili, S M Mirjalili, A. Lewis, Grey Wolf optimizer, Adv. Eng. Softw. 69 (3) (2014) 46–61.
[21] R E Precup, R C David, E M Petriu, Grey wolf optimizer algorithm-based tuning of fuzzy control systems with reduced parametric sensitivity [J], IEEe Trans. Ind. Electron. (03) (2016) 527–534.
[22] K K Choi, M M Reda, H G Taha, Punching shear strength of interior concrete slab–column connections reinforced with steel fibers, Cem. Concr. Compos. 29 (2007) 409–420.
[23] N D Gouveia, N A G Fernandes, D M V Faria etal, SFRC flat slabs punching behaviour – Experimental research, Compos. B 63 (2014) 161–171.
[24] N D Gouveia, M. Lapi, M. Orlando, Experimental and theoretical evaluation of punching strength of steel fiber reinforced concrete slabs, Struct. Concr. 19 (2018) 217–229.
[25] N D Gouveia, D M V Faria, A P Ramos etal, Assessment of SFRC flat slab punching behaviour – part II: reversed horizontal cyclic loading, Mag. Concr. Res. 71 (2019) 26–42.
[26] J Y L Voo, S J Foster, Tensile fracture of fibre reinforced concrete: variable engagement model, in: 6th Rilem symposium of fibre reinforced, concrete (FRC). Varenna (Italy); 2004, 2004, pp. 875–884.
[27] J B De-Hanai, K M A Holanda, Similarities between punching and shear strength of steel fiber reinforced concrete (SFRC) slabs and beams, IBRACON 1 (2008) 1–16.
[28] R N Swamy, S A R Ali, Punching shear behavior of reinforced slab-column connections made with steel Fiber concrete, J. Proc. 79 (1982) 392–406.
[29] P J McHarg, W D Cook, D. Mitchell, Y S Yoon, Benefits of concentrated slab reinforcement and steel fibers on performance of slab-column connections, ACI. Struct. J. 97 (2000) 225–234.
[30] Suter L. Moreillon, Punching shear strength of high performance fiber reinforced concrete slabs, in: Proc. of the 3rd FIB international congress, Washington (USA), 2010.
[31] L. Nguyen-Minh, M. Rovňák, T. Tran-Quoc, Punching shear capacity of interior SFRC slab-column connections, J. Struct. Eng. 138 (2012) 613–624.
[32] X. Shi, Machine-learning-based predictive models for punching shear strength of FRP-reinforced concrete slabs: a comparative study, Buildings (04) (2024) 14–28.

[33] P F Pan, R. Li, Y. Zhang, Predicting punching shear in RC interior flat slabs with steel and FRP reinforcements using Box-Cox and Yeo-Johnson transformations, Case Stud. Constr. Mater. (19) (2023) 23–38.
[34] A. Yaseen, Punching Shear Strength Of Steel Fiber High Strength Reinforced Concrete Slabs, Master Thesis, Erbil (Iraq): College of Engineering University of Salahaddin, 2006.
[35] X R Yu, Developing an artificial neural network model to predict the durability of the RC beam by machine learning approaches, Cases Stud. Constr. Mater. 17 (2022) 01382.
[36] Z. Liu, H. Li, G. Miao, Mapreduce-based backpropagation neural network over large scale mobile data [J], IEEE (03) (2010) 5584323.
[37] F L Luo, Multiple-page-mapping backpropagation neural network for constant tension control, IEE Proc. Electr. Power Appl. 145 (3) (2002) 239–245.
[38] Idriss Dagal, B. Akn etal, A modified multi-stepped constant current based on gray wolf algorithm for photovoltaics applications, Electr. Eng. (106) (2024) 3853–3867.
[39] X R Yu, A new method to investigate the intermediate crack-induced debonding strain, Case Stud. Constr. Mater. (17) (2022) e01646.
[40] D.P. Kingma, J. Ba, Adam: A method for stochastic optimization, Conf. ICLR. (2015).
[41] J. Kennedy, R. Eberhart, Particle swarm optimization. In: Proceedings of ICNN'95-international conference on neural networks 4, ieee, 1995, pp. 1942–1948.
[42] A M Bramm, S A Eroshenko, A I Khalyasmaa, et al., Grey wolf optimizer for RES capacity factor maximization at the placement planning stage, Mathematics 11 (11) (2023) 2545.
[43] A. Bardhan, R. Biswas, N. Kardani, M. Iqbal, P. Samui, M.P. Singh, P.G. Asteris, A novel integrated approach of augmented grey wolf optimizer and ANN for estimating axial load carrying-capacity of concrete-filled steel tube columns, Constr. Build. Mater. 337 (2022) 127454.
[44] A. Marí, A. Cladera, E. Oller, J M Bairán, A punching shear mechanical model for reinforced concrete flat slabs with and without shear reinforcement, Eng. Struct. 166 (2018) 413–426.
[45] X W Wang, W. L Tian, Z Y Huang etal, Analysis on punching shear behavior of the raft slab reinforced with steel fibers, Key. Eng. Mater. (2009) 335–340.
[46] J. Zhang, T. Zhang, Y. Zhai, P. Chen, Y. Yue, Ultimate conditions prediction and stress–strain model for FRP-confined concrete using machine learning, Arab. J. Sci. Eng. 49 (10) (2024) 14403–14428.
[47] R. Noori, Assessment of input variables determination on the SVM model performance using PCA, gamma test, and forward selection techniques for monthly stream flow prediction, J. Hydrol. 401 (2011) 177–189.
[48] James Schimert, A. Wineland, Coupling a dynamic linear model with random forest regression to estimate engine wear, Annu. Conf. PHM Soc. (2010).
[49] J.H. Chen, KNN based knowledge-sharing model for severe change order disputes in construction, Autom. Constr. 17 (2008) 773–779.
[50] F. Xiang, L. Zhang, Y. Ye, Using Pupil Diameter for psychological resilience assessment in medical students based on SVM and SHAP Model, IEEE J. Biomed. Health Inf. (28) (2024) 12–27.